Supplementary Information (SI) for Journal of Materials Chemistry A.

Solvent-free Lithium-Ion Battery Electrode with Ultrahigh Loading Using Reactive Epoxy Nano Binder

Pingwei Zhu,[ab] Siqi Liu,[ab] Lei Zhao,[ab] Li Liu,[ab] Yudong Huang,[ab] Jun Li*[ab] and Fujun Li*[c]

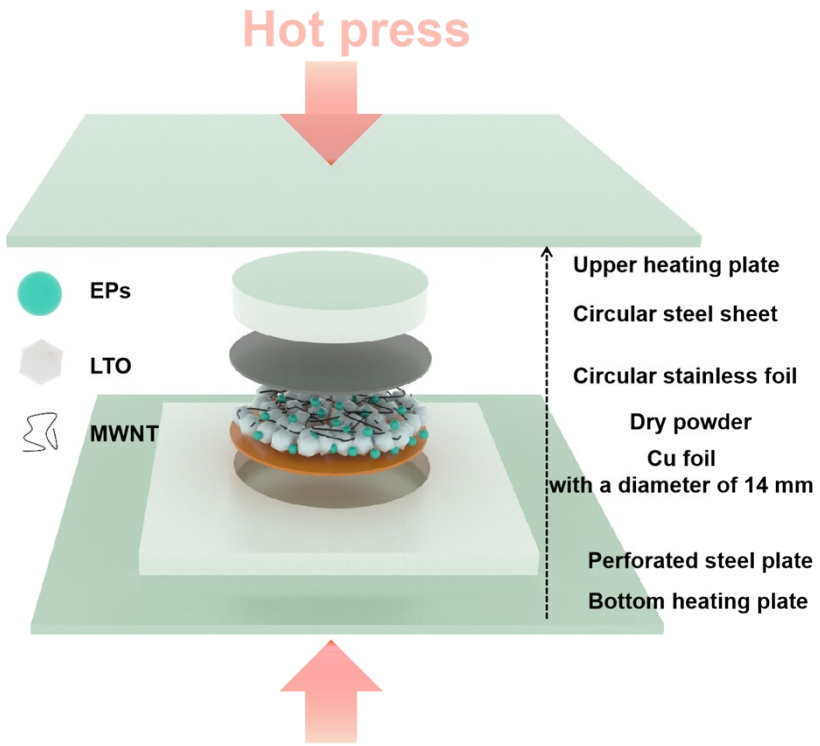

Fig. S1. Schematic diagram of a simple one-step method for the preparation of dry electrodes.

[a]School of Chemistry and Chemical Engineering, Harbin Institute of Technology, Harbin 150001, China. E-mail: junlihit@hit.edu.cn
[b]MIIT Key Laboratory of Critical Materials Technology for New Energy Conversion and Storage, Harbin Institute of Technology, Harbin 150001, China. E-mail: junlihit@hit.edu.cn
[c]Frontiers Science Center for New Organic Matter, Key Laboratory of Advanced Energy Materials Chemistry (Ministry of Education), College of Chemistry, Nankai University, Tianjin 300071, China. E-mail: fujunli@nankai.edu.cn

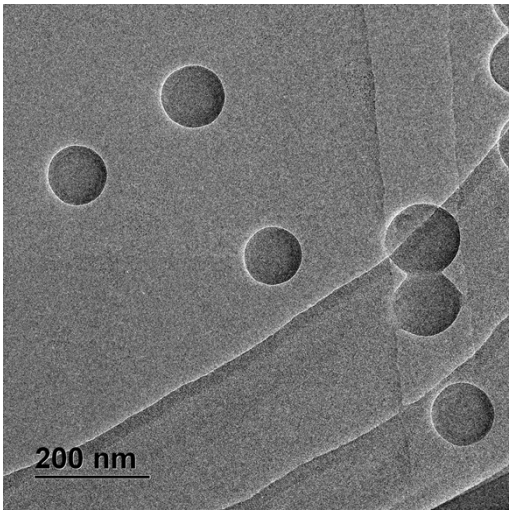

Fig. S2. TEM image of EPs.

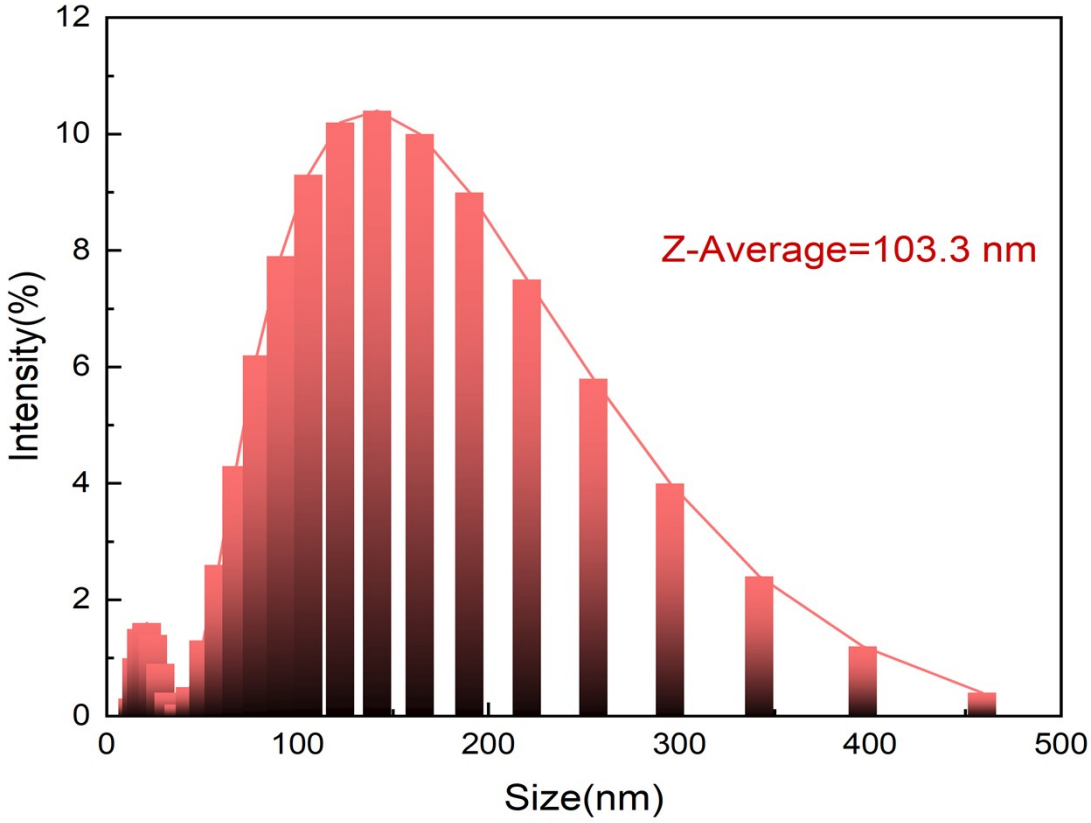

Fig. S3. Laser particle size scanning curve of EPs.

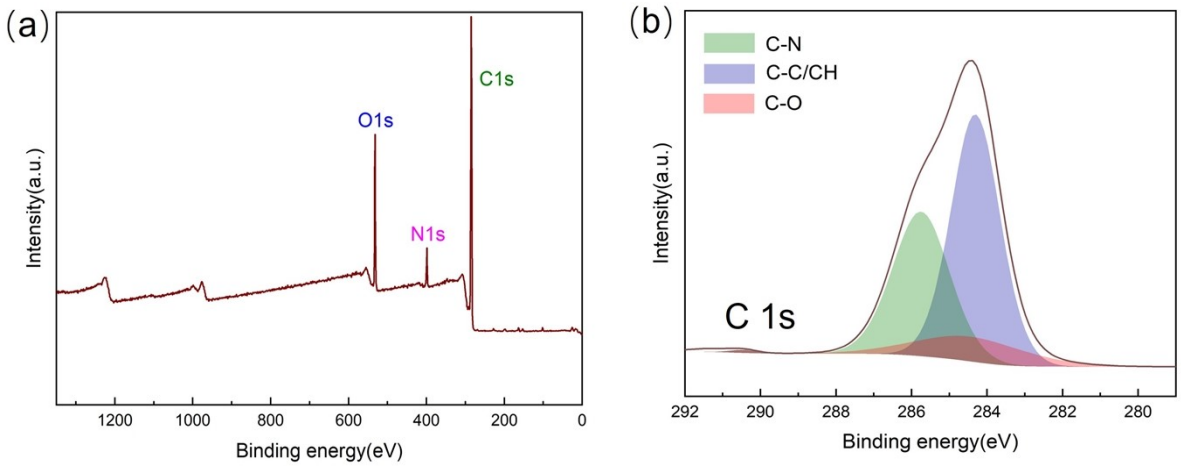

Fig. S4. (a) XPS spectra of EPs. (b) XPS C 1s spectra of EPs.

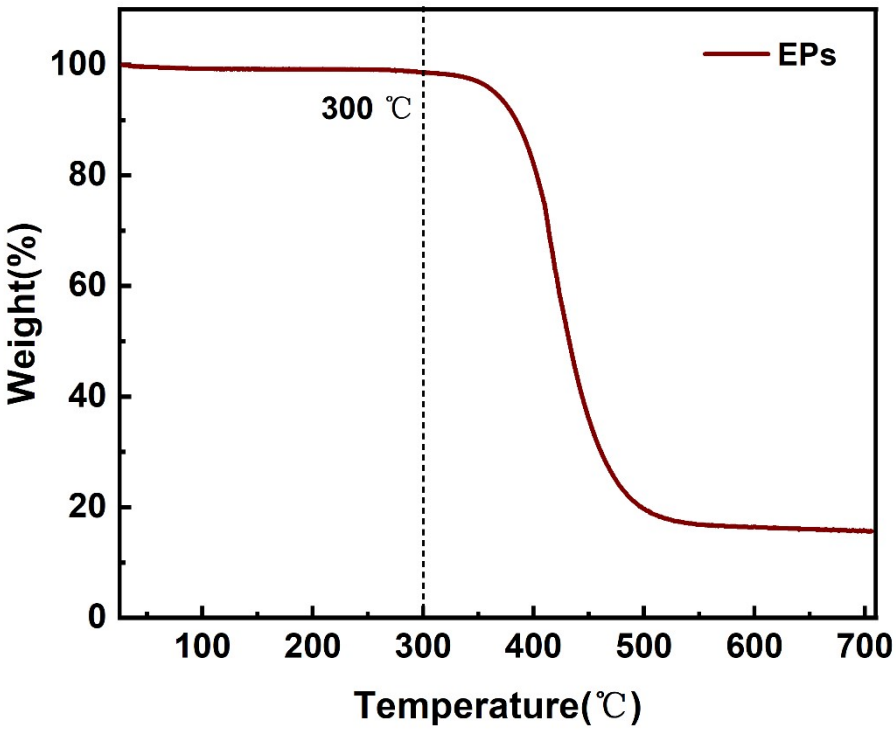

Fig. S5. TGA curve of EPs

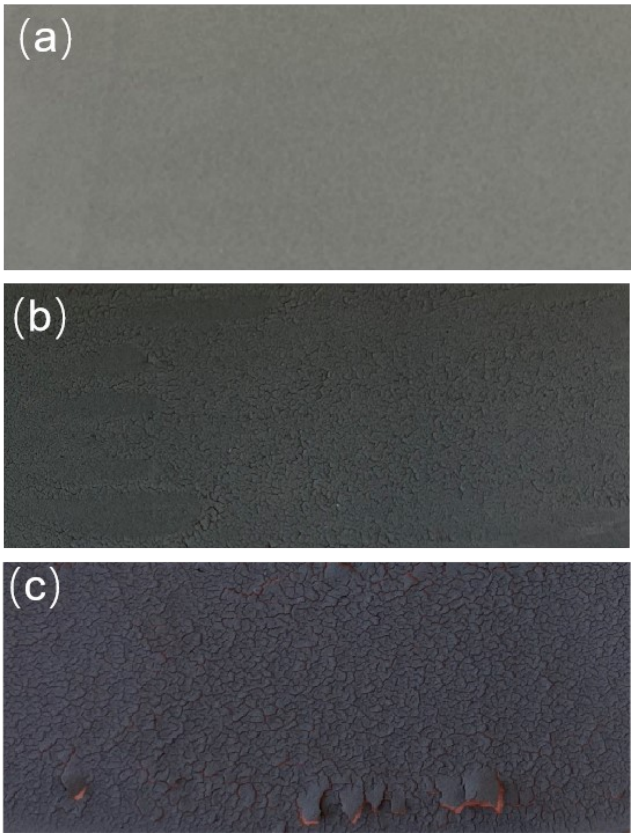

Fig. S6. (a) Thin electrodes prepared using a 150 μm applicator. (b) Thick electrodes prepared in a single coating using a 300 μm applicator. (c) Thick electrodes prepared by double coating using a 150 μm size applicator.

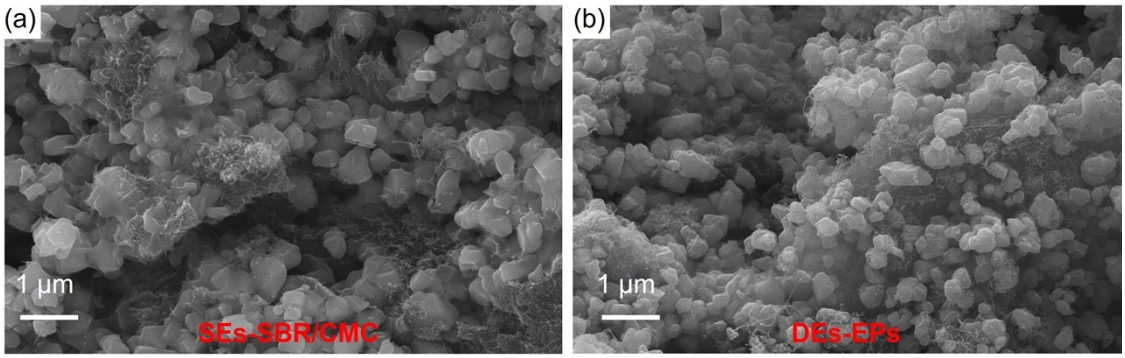

Fig. S7. (a) Cross-sectional morphology of SEs. (b) Cross-sectional morphology of DEs.

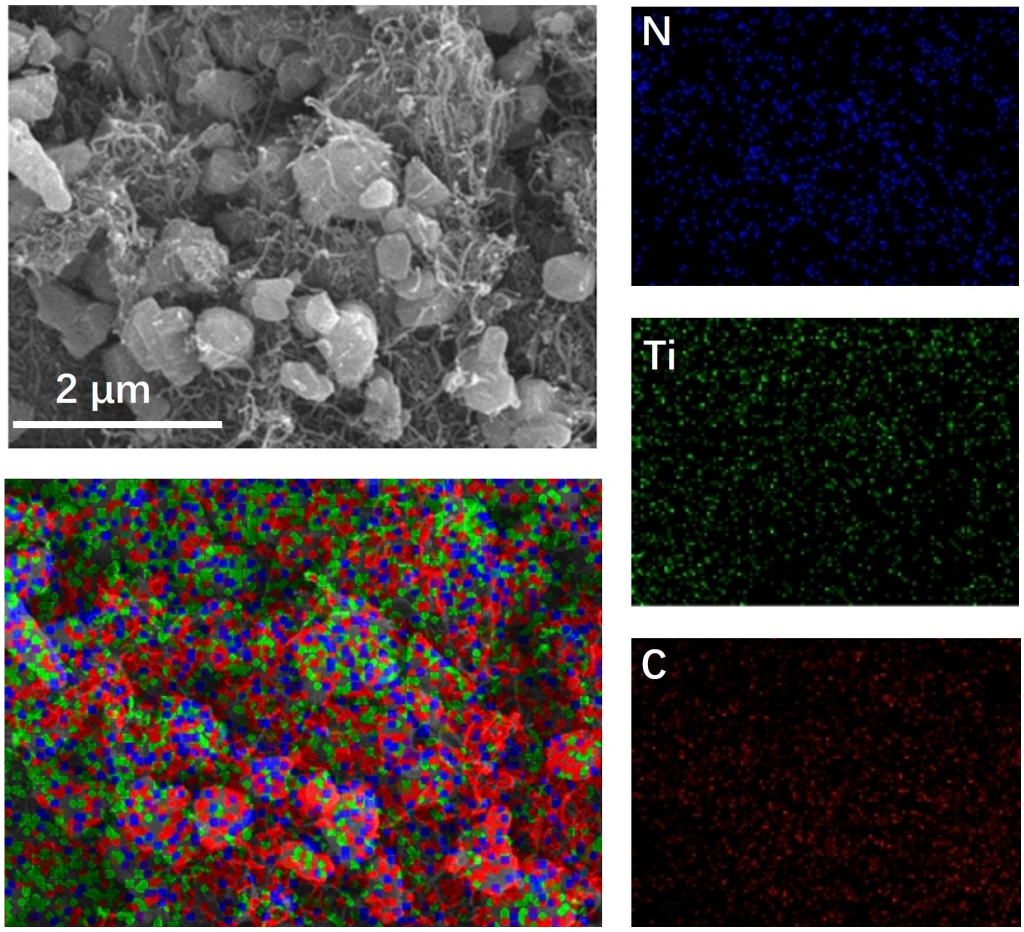

Fig. S8. The SEM and elemental mapping images of the DEs.

Table S1 Swelling rate of electrodes prepared by different binders in electrolyte

Anode	Swelling rate (%)	
	24 h	48 h
SEs-SBR/CMC	21.29	25.16
DEs-PVDF	37.77	41.49
DEs-EPs	11.81	14.52

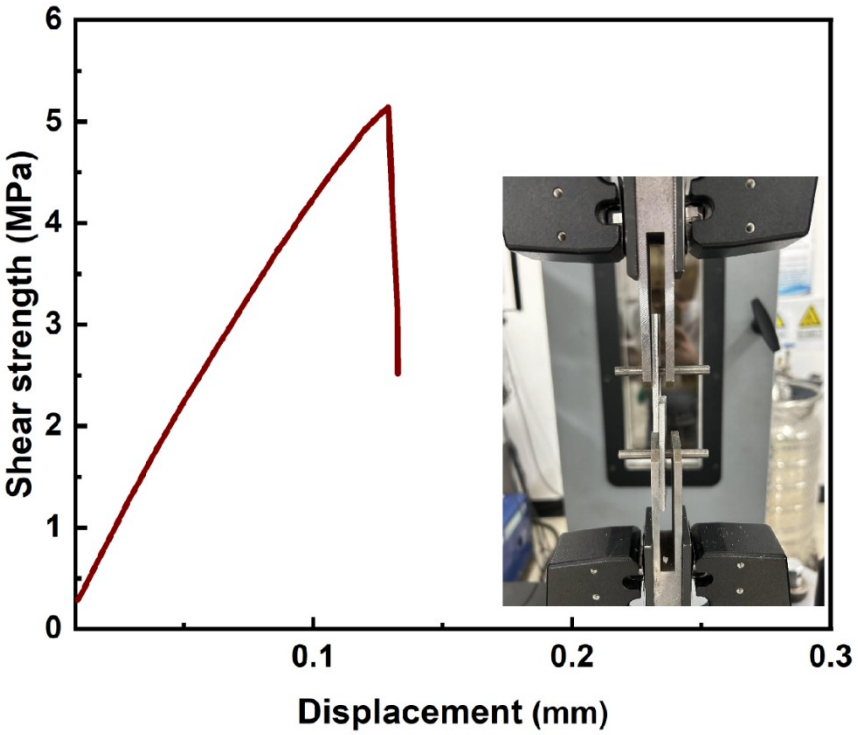

Fig. S9. Shear strength-displacement curve of EPs

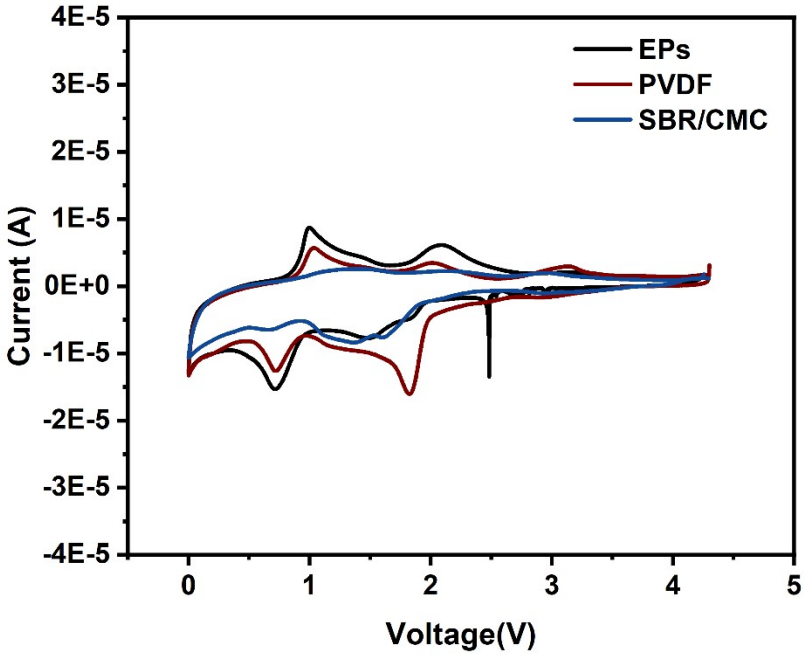

Fig. S10. CV curves at a scan rate of 0.2 mV s^{-1} between 0 and 4.3 V.

Text S1

The diffusivity coefficient of Li^+ (D_{Li^+}) can be calculated based on the following Equation (1):

$$D_{Li^+} = \frac{R^2T^2}{2A^2n^4F^4C^2\sigma^2} \quad (1)$$

Where R is the gas reaction constant with a calculated value of 8.314 J mol^{-1} K^{-1}, T represents the absolute thermodynamic temperature degree (298 K), F refers to the Faraday constant (96500 C mol^{-1}), A is the area of the assembled electrode, n represents the number of electrons transferred in the Ti^{4+}/Ti^{3+} redox reaction (1), C refers to the concentration of Li^+ in the crystal lattice (4.17×10^{-3} mol cm^{-3}), and σ is the Warburg region.

Uniform dispersion of conductive agents is critical to cycling performance for the high mass loading electrodes. It can be found that MWNT in both HDEs are evenly dispersed around the active material without visible agglomeration, which confirms the universality of the dry-process in this work (Fig. S6).

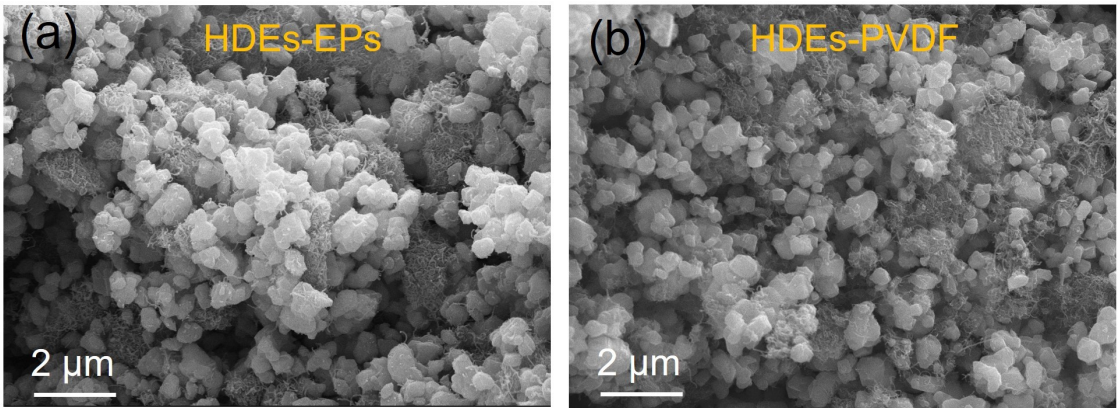

Fig. S11. (a) Cross-sectional morphology of HDEs-EPs. (b) Cross-sectional morphology of HDEs-PVDF.

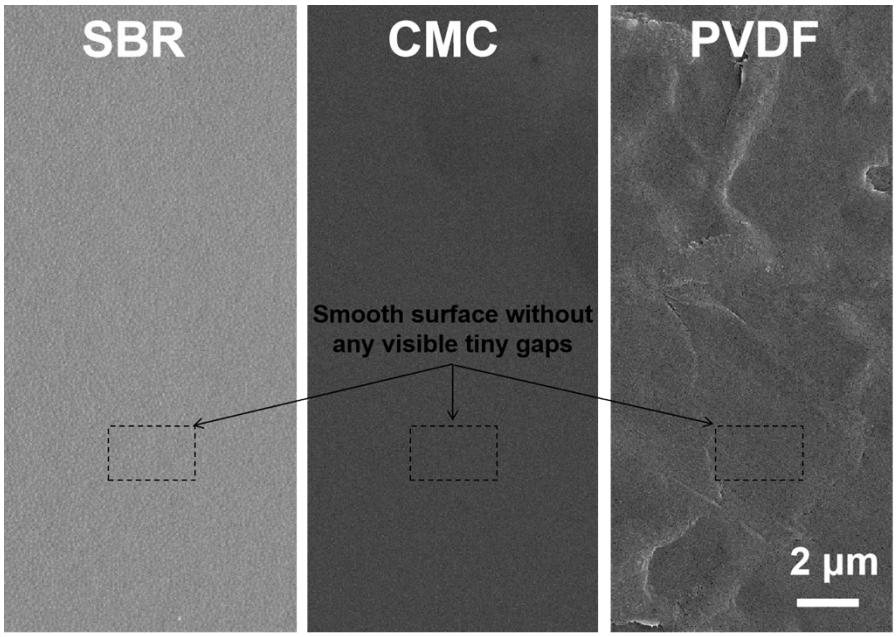

Fig. S12. SEM image of the self-bonding process of SBR, CMC and PVDF.

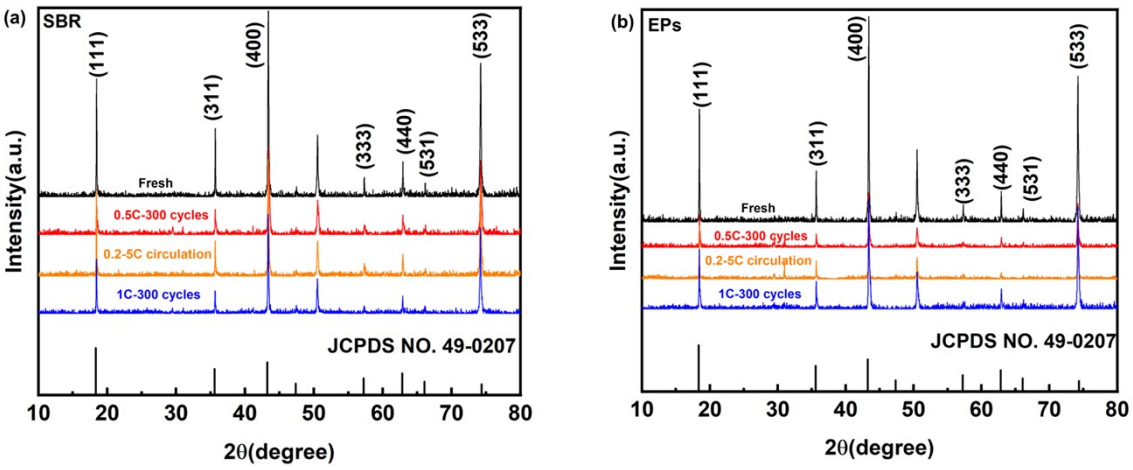

Fig. S13. XRD patterns of (a) fresh SBR electrode and cycled SBR electrode, (b) fresh EPs electrode and cycled EPs electrode

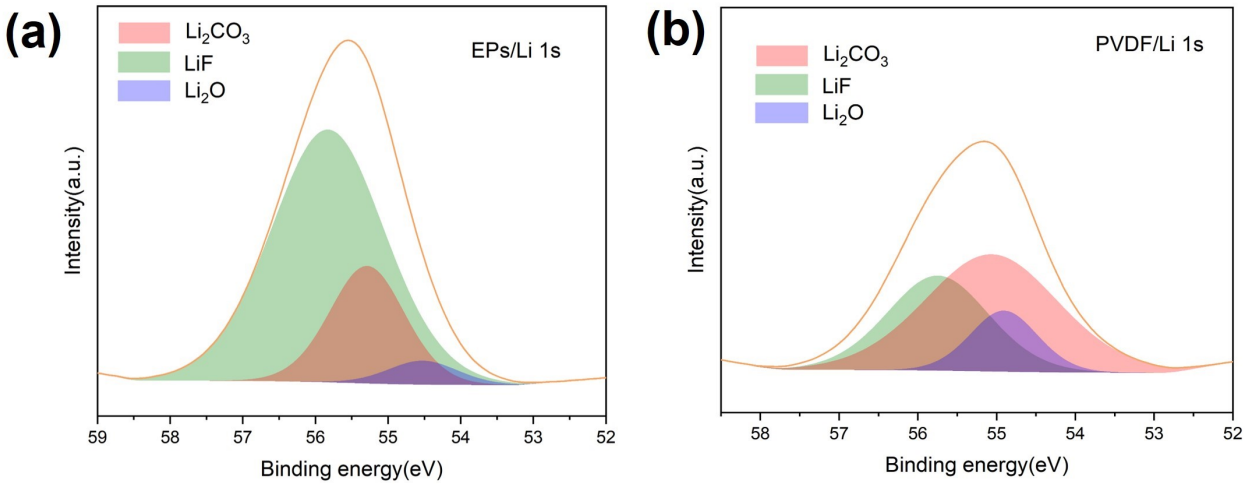

Fig. S14. XPS Li 1s spectra of (a) HDEs-EPs and (b) HDEs-PVDF after 350 cycles.

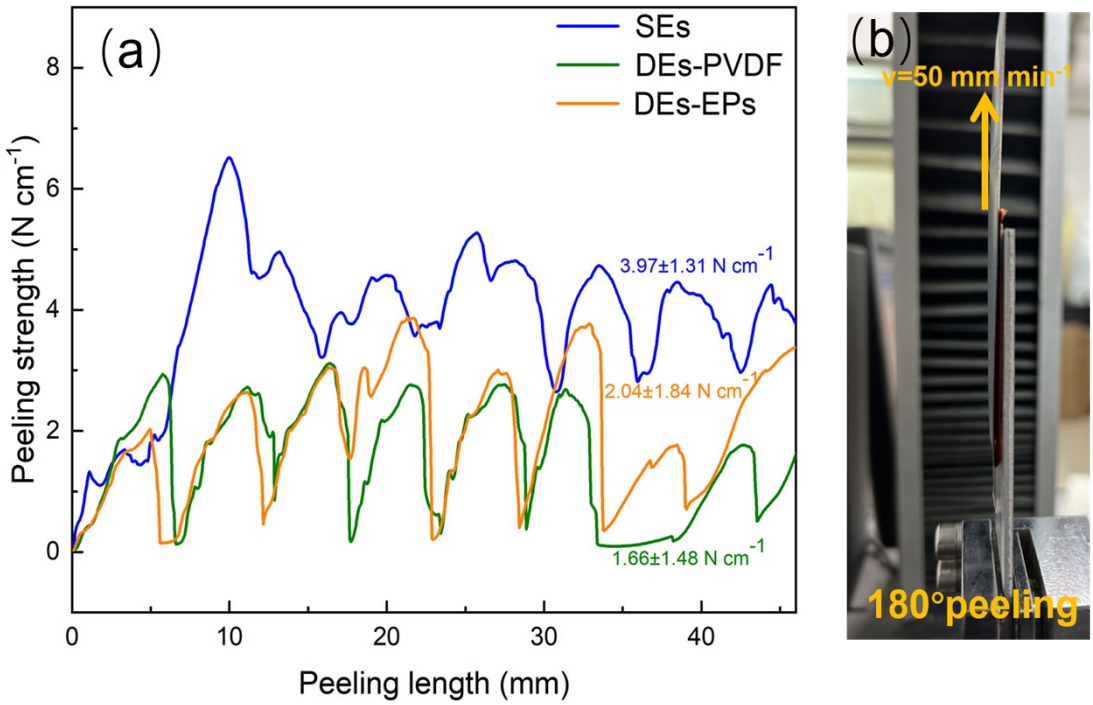

Fig. S15. (a) Adhesion force of the SEs, DEs-PVDF and DEs-EPs, which was characterized using (b) 180° peel-off test

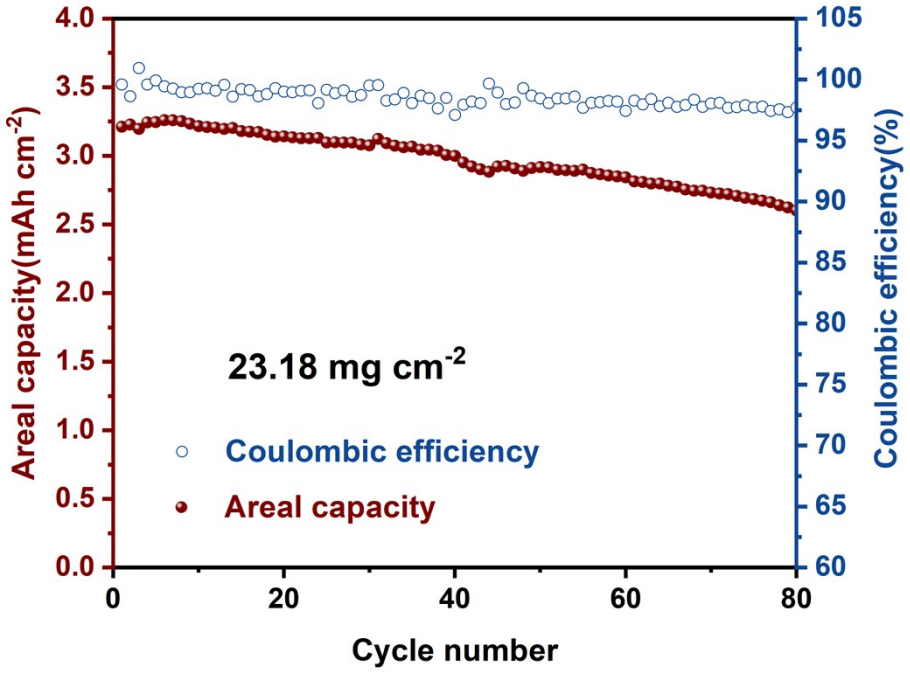

Fig. S16. Cycling performance of HDEs-EPs-NCM811.

Supplementary references

[1] W.D. Connor, S. Arisetty, K.P. Yao, K. Fu, S.G. Advani, A.K. Prasad, Analysis of solvent-free lithium-ion electrodes formed under high pressure and heat, J. Power Sources 546 (2022) 231972.

[2] C. Lv, W. He, J. Jiang, E. Zhen, H. Dou, X. Zhang, Structure optimization of solvent-free $Li_4Ti_5O_{12}$ electrodes by electrostatic spraying for lithium-ion capacitors, J. Power Sources 556 (2023) 232487.

[3] H. Zhou, M. Liu, H. Gao, D. Hou, C. Yu, C. Liu, D. Zhang, J.-c. Wu, J. Yang, D. Chen, Dense integration of solvent-free electrodes for Li-ion supercabattery with boosted low temperature performance, J. Power Sources 473 (2020) 228553.

[4] M. Al-Shroofy, Q. Zhang, J. Xu, T. Chen, A.P. Kaur, Y.-T. Cheng, Solvent-free dry powder coating process for low-cost manufacturing of $LiNi_{1/3}Mn_{1/3}Co_{1/3}O_2$ cathodes in lithium-ion batteries, J. Power Sources 352 (2017) 187-193.

[5] E. Zhen, J. Jiang, C. Lv, X. Huang, H. Xu, H. Dou, X. Zhang, Effects of binder content on low-cost solvent-free electrodes made by dry-spraying manufacturing for lithium-ion batteries, J. Power Sources 515 (2021) 230644.

[6] D.J. Kirsch, S.D. Lacey, Y. Kuang, G. Pastel, H. Xie, J.W. Connell, Y. Lin, L. Hu, Scalable dry processing of binder-free lithium-ion battery electrodes enabled by holey graphene, Acs Appl. Energy Mater. 2 (2019) 2990-2997.

[7] B.A. Walker, C.O. Plaza-Rivera, S.-S. Sun, W. Lu, J.W. Connell, Y. Lin, Dry-pressed lithium nickel cobalt manganese oxide (NCM) cathodes enabled by holey graphene host, Electrochim. Acta 362 (2020) 137129.